Experimental Study of Symmetric Microstrip Bends and Their Compensation

RENE J. P. DOUVILLE, MEMBER, IEEE, AND DAVID S. JAMES, MEMBER, IEEE

Abstract—**An experimental study of microstrip bends is described. For right-angle corners, equivalent circuit parameters covering a wide range of frequencies, linewidths, and permittivities are presented and compared with the limited theoretical values available. The influence of mitering or rounding of the corner was investigated, and useful empirical expressions are given for the optimum miter.**

I. Introduction

ALTSCHULER AND OLINER [1], [2] have investigated right-angle bends in stripline both analytically, using a Babinet equivalence to waveguide, and experimentally. Campbell [3] extended the analysis to the special case of a 45°, 50 percent miter. Silvester and Benedek [4] have numerically evaluated the excess capacitance, and Gopinath and Easter [5], Horton [6], and Thomson and Gopinath [7] the excess inductance associated with the microstrip right-angle bend. In all cases, the values obtained are quasistatic only. Wolff and Menzel have used mode-matching techniques to compute frequency dependent S-parameters for an unsymmetrical right-angle bend [8]. No theoretical results are available for designing matched bends.

To date, only limited experimental results have been reported, most notable being those of Easter *et al.* [9]–[11], and Kelly *et al.* [12], all for the special case of lines on substrates having $\varepsilon_r \doteq 10$.

For these reasons, measurements were undertaken to more adequately characterize the symmetric microstrip right-angle bend over a wide range of useful impedances, substrate permittivities and frequencies. The possible improvements provided by geometrical modification to the outer portion of the right-angle bend, including a 45° miter, were investigated. The miter geometry which minimizes the bend VSWR was determined over a useful range of practical parameters.

Fig. 1(a)–(c) define those parameters of the microstrip and bend which will be discussed. Although the lumped-element equivalent circuit of Fig. 1(g) gives more physical insight into the nature of the discontinuity, that of Fig. 1(f) is of more practical convenience in circuit design. The reference planes T_1 and T_2, taken to be at the inside edges of the microstrip lines, do not completely enclose the discontinuity fields. Therefore, it is possible for the equivalent circuits to contain negative elements. Originally, it was planned to include allowance for radiation from the bends in the form of a resistive element. However, preliminary measurements indicated the radiation contribution to our measurements to be essentially negligible. Again this should not be construed to mean that under all circumstances the radiation associated with the bend will remain insignificant.[1]

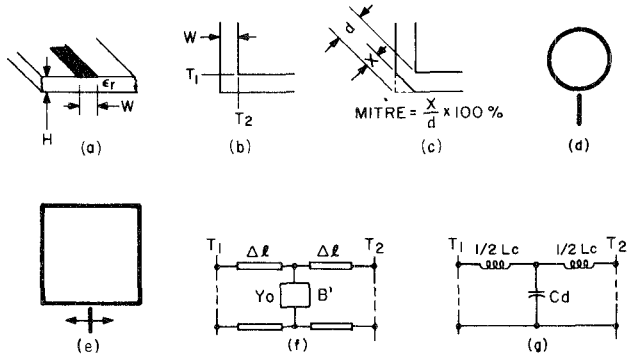

Fig 1. (a) Microstrip geometry. (b) Right-angle bend. (c) Mitered bend. (d) Round-reference loop. (e) Square loop with movable probe. (f) Bend equivalent circuit. (g) Alternative lumped-element equivalent circuit.

II. Experimental Methods

A. Resonant Loop

The method used in the majority of the measurements was first described by Douville and James [15], and later used by Hoefer and Chattopadhyay to evaluate shunt posts in microstrip [16]. It may briefly be described as follows. A standing wave pattern is excited on a square microstrip loop resonator (Fig. 1(e)). Very light coupling ($\beta < 0.05$) is used, thereby minimizing any influence of the coupling strip on the loop-resonant frequency. With the launcher at midpoint and for all even harmonic resonances, voltage nodes or antinodes are located simultaneously at all four corners. If voltage nodes exist at the corners, the voltage across B' is zero, and thus B' has no effect on the total electrical length and resonant frequency of the loop. If the coupling point is moved off center about one quarter wave such that a voltage

Manuscript received May 9, 1977; revised September 30, 1977

R. J. P. Douville is with the Communications Research Centre, Department of Communications, Ottawa, Ont., K2H 8S2, Canada.

D. S. James was with the Communications Research Centre, Ottawa, Ont., Canada. He is now with Ferranti Solid-State Microwave, Manchester, England.

[1] Some idea of the magnitude of the radiated power P_{rad} for a 90° bend may be obtained from Lewin [13] as modified by Hammerstad [14]; $P_{rad}/P_{inc} \sim 0.07[H_{(mm)} f_{(GHz)}]^2/Z_0 \varepsilon_{eff}$, where P_{inc} is the power incident on the corner and the other symbols have their usual meaning. For the fairly extreme example of a 25-Ω line on a 0.635-mm substrate with $\varepsilon_r \simeq 2.5$, the loss would be expected to be about 0.35 dB at 12 GHz.

0018-9480/78/0300-0175$00.75 © 1978 IEEE

antinode exists at the corner, B' has a field maximum across it causing a reduction in the loop-resonant frequency.

By measuring these two frequencies, the value of the normalized discontinuity susceptance B' may be computed as

$$B' = \frac{B}{Y_0(f_n)} = 2 \tan\left(\frac{\pi k}{4} \cdot \frac{f_n - f_a}{f_n}\right) \tag{1}$$

where

f_n frequency with a node at the corner,
f_a frequency with an antinode at the corner,
k harmonic number (only even values used),
$Y_0(f_n)$ the characteristic admittance at f_n,
B unnormalized discontinuity susceptance.

To obtain the equivalent electrical length of the corner, it is necessary to measure the resonant frequency f_r of a circular loop fabricated on the same substrate and having a mean circumference equal to twice the length of one side of the square loop (Fig. 1(d)). The value of $\Delta\ell$ may be obtained as

$$\Delta\ell = \ell_c\left(\frac{f_r - f_n}{4f_n}\right) \tag{2}$$

where

$\Delta\ell$ half the total bend equivalent length between planes, T_1 and T_2,
f_r round loop-resonant frequency,
ℓ_c mean circumference of round loop.

The element values appropriate to the equivalent circuit of Fig. 1(f) and those for the lumped-element equivalent circuit of Fig. 1(g) may be compared by equating the corresponding $ABCD$ matrices, thereby leading to the following expressions:

$$\frac{B'}{2\pi f} = \frac{(B_1' - \sin 2\theta)\, s^2\, \theta}{2\pi f} \xrightarrow{f \to 0} C_d - 2\Delta\ell C_\infty \tag{3}$$

$$L_c = 2\Delta\ell L_\infty \tag{4}$$

where

θ $2\pi\Delta\ell/\lambda g = (2\Delta\ell/H)(\pi H f \sqrt{\varepsilon_{\text{eff}}}/c)$,
C_∞, L_∞ microstrip capacitance and inductance per meter,
B_1' $\omega C_d Z_0(f)$.

For this discontinuity, the second term in (3) typically is not small in comparison to the first. The designer is therefore cautioned against simply estimating the expected mismatch at frequency f from a normalized susceptance equal to $2\pi f C_d Z_0(f)$.

B. Meander Line

Some results were additionally obtained by use of swept frequency return loss measurements on circuits consisting of a number of bends arranged in meander-line fashion. With half-wavelength spacing between bends it is possible to obtain reasonably accurate data for the shunt susceptance of the discontinuity, but not for the corresponding reference plane shift $\Delta\ell$. For small bend VSWR's, the sign of the shunt susceptance was verified by means of impedance measurements with a network analyzer. Most of these tests were undertaken on 0.635-mm thick substrates.

III. Resonant-Loop Experiments

All experiments were performed on oversize 30 × 30 × 0.5-cm substrates. The errors encountered by Stephenson and Easter in their tests and attributed to dimensional inaccuracies aggravated by the very small dimensions of conventional microstrip were minimized by scaling up in this fashion. As a consequence, the measurements were performed over the frequency range 0.2–3 GHz, so that, by suitable rescaling, the data may be applied to the much higher frequencies generally encountered in microwave integrated circuits. For example, for a typical alumina substrate of thickness 0.635 mm, the scale factor is 8, effectively extending the results to 24 GHz.

The substrates were mounted in a large metal box. The type N launcher, mounted on a slider, was positioned along one side of the square resonator such that either one or the other of the two resonances was suppressed. To avoid the possibility of a changing physical environment influencing the measurements, most B' and $\Delta\ell$ measurements reported here were obtained with the box completely closed. The inevitable box and surface modes were suppressed by judicious use of absorber material.

Preliminary measurements of the round loop-resonance frequency revealed that Stycast[2] having an ε_r of about 10 possesses a temperature coefficient of capacitance of about 500 ppm/°C, so that a change of only a few degrees Celsius is accompanied by a measurable change in frequency. For purposes of calculation of B', this change was inconsequential. However, since the frequencies used in obtaining $\Delta\ell$ are taken after a fabrication cycle, changes of only a few degrees Celsius between measurements on the square-loop and round-loop resonators may have a substantial influence. In order to minimize this effect, all measurements were performed at a controlled temperature of 19 ± 2°C.

To justify the use of the arithmetic mean circumference of the round-loop resonator in the determination of $\Delta\ell$, the ε_{eff} determined using a 50-Ω linear resonator constructed on the same Stycast substrate as a round one was measured and is shown in Fig. 2.[3] The effect of the round-loop curvature is obviously negligible. It was also verified both experimentally and analytically that for the coupling gap used, the influence of the coupling capacitance on the B' and $\Delta\ell$ values was negligible.

This method, similar to that described by Easter and Stephenson [9] minimizes the problems encountered in measuring the reflection and transmission properties of discontinuities through transitions or launchers. The characteristics of such transitions are generally poor and

[2] Emerson and Cuming, Inc.

[3] The Z_0 values indicated throughout were obtained using $Z_0(f) = Z_0(\varepsilon_{\text{eff}\,0}/\varepsilon_{\text{eff}})$ where $\varepsilon_{\text{eff}\,0}$ was obtained using Hammerstad [17] and ε_{eff} is that measured and appropriate to X-band and 0.635-mm substrates. Note that although these values of $Z_0(f)$ do not have any substantial effect on the results, care should be exercised in using them in an absolute sense as suggested by Schmitt and Sarges [22].

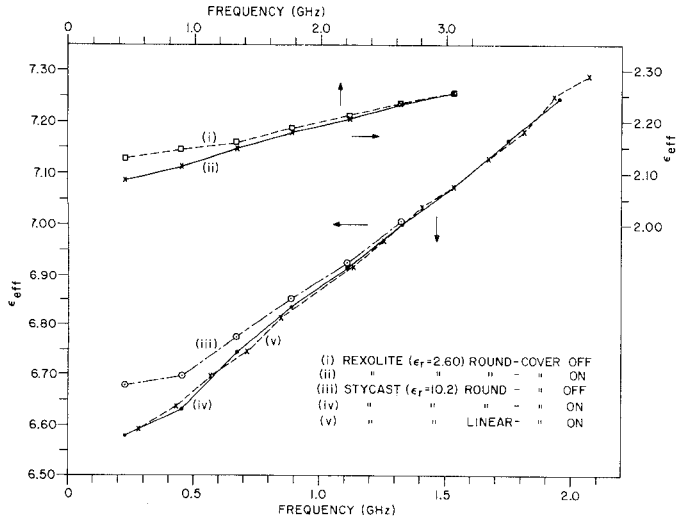

Fig. 2. Measured frequency dependence of ε_{eff} for round and linear 50-Ω (nom.) resonators on Rexolite and Stycast, $H = 5.08$ mm.

unrepeatable. However, the resonant loop method used here has the advantage over that used by Stephenson and Easter in that it eliminates the necessity of interpolating between alternate harmonics in order to calculate B'. This interpolation procedure is rendered inaccurate by virtue of the strongly dispersive behavior of microstrip. In the method used here, both f_n and f_a are measured at every harmonic, thus eliminating the need for any interpolation. In fact, by interpolating between even harmonics, it is possible with this method to obtain B' values at the odd harmonics as well. An attempt to do so, however, demonstrated that the interpolation process is sufficiently inaccurate to introduce significant scatter in the results.

IV. Results

A. Bend Equivalent Electrical Length

Fig. 3(a) and (b) illustrate curves of normalized $\Delta\ell$ measurements as functions of frequency and percentage miter for nominally 50-Ω lines on Stycast of $\varepsilon_r = 10.8$ and Rexolite of $\varepsilon_r = 2.6$. Similar curves were obtained for 33-Ω and 76-Ω lines on $\varepsilon_r = 10.8$ as well as for 43-Ω lines on $\varepsilon_r = 5$.

Using a finite-difference computer program as well as a program based on Smith's analysis [19], the effect of the proximity of the sidewalls and lid on the quasistatic value of ε_{eff} was calculated. In Fig. 2 the measured effect of the lid ($5.5H$ above the substrate) is apparent and, in the low frequency limit, in good agreement with that predicted. The computations also indicated that in most cases, even though the sidewall proximity is much greater for the square loop than for the round, there is no substantial effect on the $\Delta\ell$ values if the lid is installed. However, in the sole case of 50-Ω lines on $\varepsilon_r = 10.8$, a change in ε_{eff} of approximately 0.7 percent from that with the sidewalls far removed was computed. Although this has no effect on the B' values, it suggests an upward adjustment of the $2\Delta\ell/H$ curves in Fig. 3(a) by $+0.15$. Since the frequency dependence of this correction could not be readily ascertained, and since the

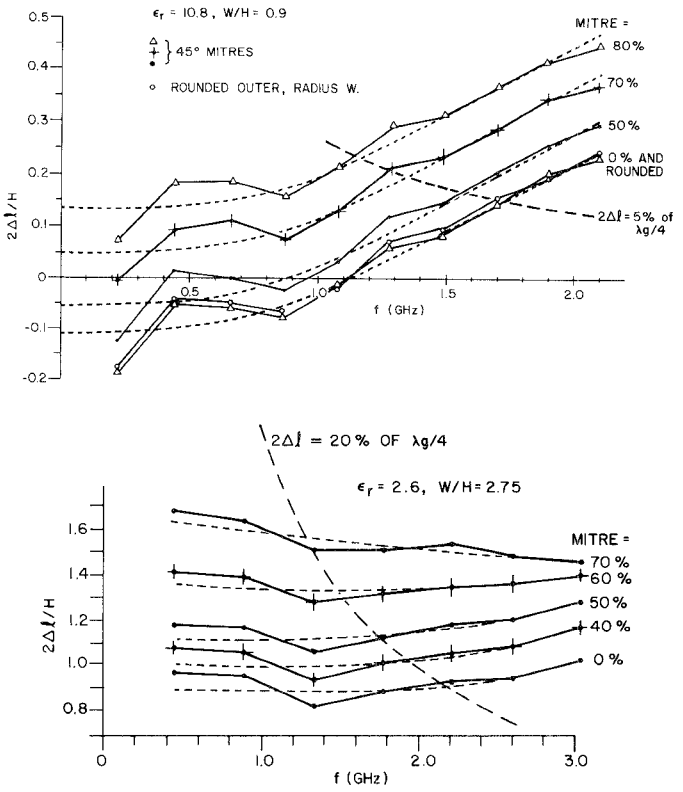

Fig. 3. Frequency dependence of normalized bend electrical length for various miters. Lines are 50 Ω (nom.) on 5.08-mm thick Stycast (a), and Rexolite (b).

measured dispersive ε_{eff} curves indicate a definite frequency dependence of the lid proximity effect, the correction has not been incorporated into the curves of Fig. 3(a).

Since the computed effects of the proximity of the lid and sidewall on ε_{eff} are quite small, it is considered that the discontinuity fields and therefore the B' and $\Delta\ell$ values will not be substantially influenced.

It may be noted that the bend electrical length can become a significant fraction of a quarter wavelength, as graphically illustrated by the dashed curves in Fig. 3(a) and (b). Fig. 3(a) and (b) also reveals that a commonly used practice, that of rounding the outer corner of the bend, has essentially no effect on $\Delta\ell$, as expected. Additionally, it is apparent that substantial mitering may take place before the bend electrical length is greatly influenced.

The measured frequency dependence of $\Delta\ell$ appears to be more pronounced for $\varepsilon_r = 10.8$ than for the lower ε_r's, although at least some of this dependence may be attributed to the proximity effect described above. Although some possible reasons for the cyclical nature of the data of Figs. 3 and 4 have been investigated, the cause is not understood, and therefore, to facilitate ready comparison with published results, the dotted line approximations to the data have also been drawn.

B. Bend Susceptance

Fig. 4(a) and (b) shows the measured values of the normalized bend susceptance for nominally 50-Ω lines on

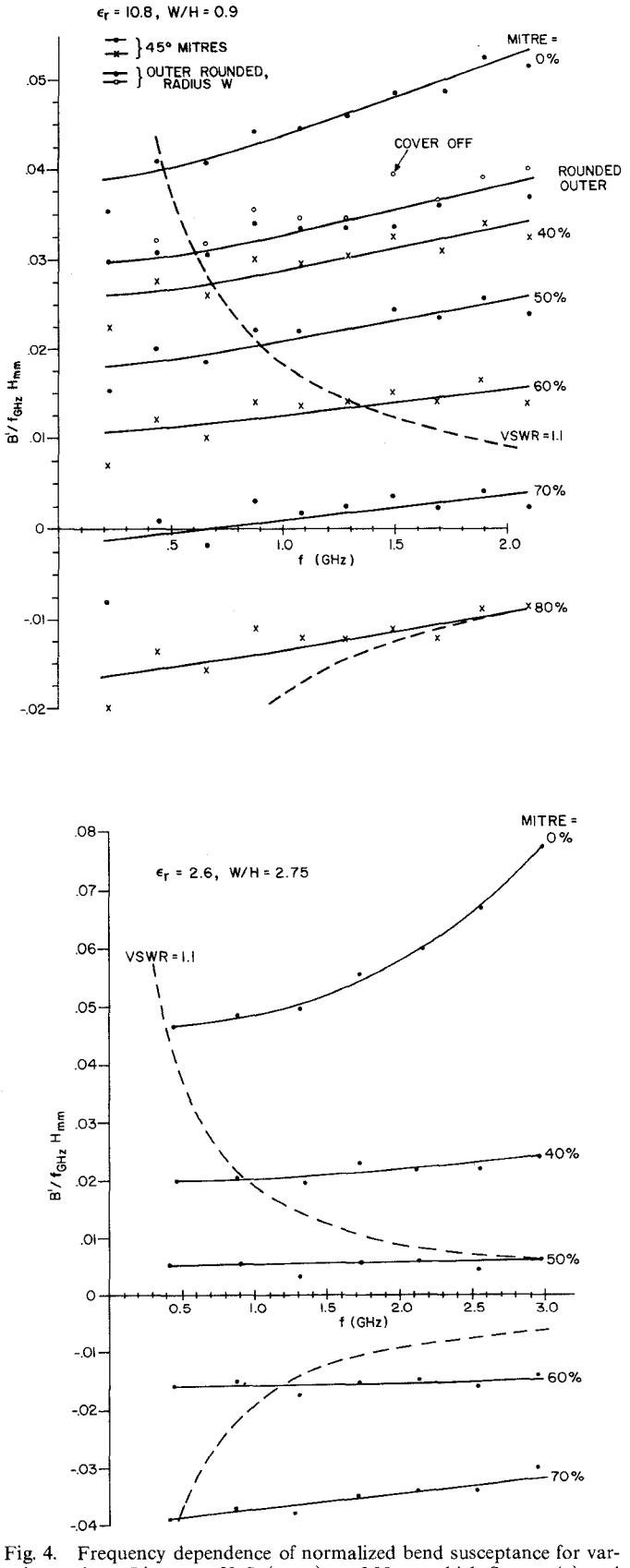

Fig. 4. Frequency dependence of normalized bend susceptance for various miters. Lines are 50 Ω (nom.) on 5.08-mm thick Stycast (a), and Rexolite (b).

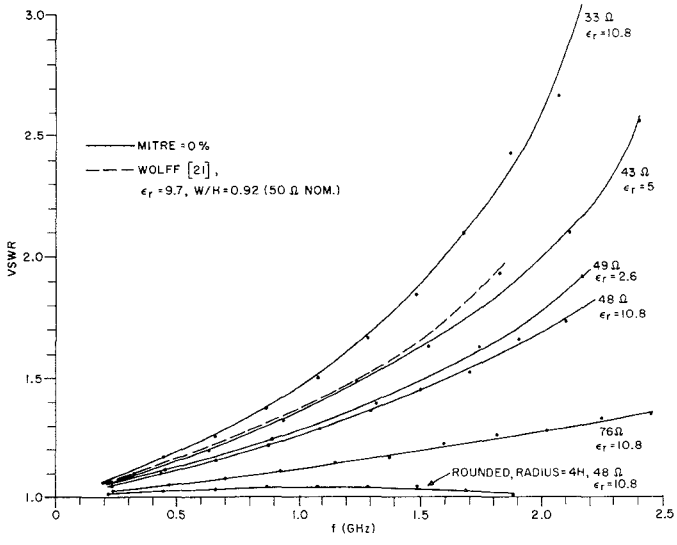

Fig. 5. Variation of VSWR with frequency for unmitered 90° bends (f = 1.5 GHz).

ε_r = 10.8 and 2.6 as functions of both frequency and percentage miter. Again, similar curves were obtained for other geometries and ε_r's. As expected, as the miter percentage is increased the bend susceptance eventually becomes inductive; the point at which this transition takes place is the optimum miter. In these and all other cases studied, substantial mitering (~ 50 percent) is required before any appreciable reduction in the bend susceptance occurs. Also from Fig. 4(a) it can be seen that rounding the outer perimeter of the bend yields little improvement over that of the unmitered bend. In all cases examined, the frequency dependence of B'/fH is pronounced only for the unmitered case and is almost totally eliminated as the optimum miter is approached. Curves of constant VSWR = 1.1 are superimposed on Fig. 4(a) and (b) and illustrate that even for frequencies as high as 1.5 GHz (12 GHz on 0.635 mm), the tolerance of the optimum miter is quite substantial.

The importance of mitering is graphically illustrated in Fig. 5 where the VSWR of the unmitered bends is illustrated for several ε_r and Z_0 cases studied. In many practical cases, the mismatch can be seen to become severe at higher frequencies. Although not always convenient, a 90° arc can sometimes be used satisfactorily as an alternative to an abrupt bend, and Fig. 5 includes performance obtained with a relatively large arc of mean radius $4H$ in a 48-Ω line on ε_r = 10.8.

C. Comparison with Published Data

For the electrical length component, Fig. 6 shows that reasonably good agreement is observed between measured data extrapolated to zero-frequency and the theoretical quasi-static data of Thomson and Gopinath [7]. The data points for the dotted curve represent similarly extrapolated values associated with the optimum miter; the optimum miter will be shown in Section V to be dependent on W/H only. For the 50-percent miter case the $\Delta\ell$ results derived from Campbell's curves [3] along with the Babinet equiv-

TABLE I
COMPARISON OF MEASURED AND CALCULATED VALUES FOR B'

		$f \to 0$ [3,6]				$f = 1.5$ GHz [3,6]			
ε_r	W/H	Zo (Ω)	UPWM[1]	B&S[2]	Exp't	Zo(f) (Ω)	UPWM[1]	B&S[2]	Exp't
2.6	2.75	50	5.4	5.1	4.6	49	5.5	5.2	5.3
5.0	2.15	44	5.7	5.2	5.3	43	6.5	6.0	6.5
10.1	0.88	52	5.3	4.7	4.2	50	5.3	4.7	4.6
10.8	0.9	50	5.5	5.0	3.9	48	5.6	5.1	4.9
10.8	1.75	35	7.6	7.1	6.3	33	8.0	7.5	8.3
10.8	0.28	78	3.3	2.8	1.9	76	3.4	2.9	2.3
15[4]	0.48	55.5	4.8	4.2	--	52.5	4.8	4.2	3.7
25[5]	0.33	49.5	5.2	--	--	46.5	5.4	--	2.7
		$[B'/f_{(GHz)}H_{(mm)}] \times 100$							

Notes: 1. Ref. [11]
2. " [4]
3. From (3) & (4). $\Delta\ell$ obtained from [7]. Rescaled for H as per notes 4 or 5 for $f \neq 0$.
4. H = 0.635 mm
5. H = 1.52 mm
6. Zo(f) & $\varepsilon_{eff}(f)$ computed from Hammerstad [17] and Getsinger [18].

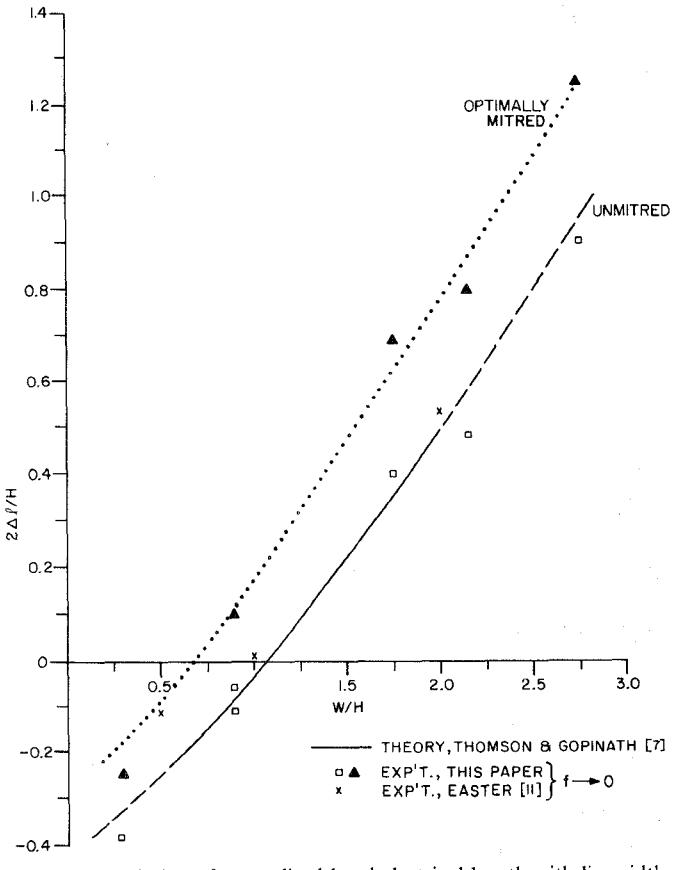

Fig. 6. Variation of normalized bend electrical length with linewidth.

alence between parallel-plate guide and microstrip [20] are quite misleading.

Table I presents a comparison of the measured susceptance results for the 0-percent cases with theoretical data available. The simple expression $C_d = C_\infty W$, particularly convenient for practical circuit design, may be obtained by use of the simple uniform plane wave model (UPWM) [11]. Such computed results, when used in (3) along with the $2\Delta\ell/H$ values of Fig. 6, yield values of the shunt susceptance component B' which are in approximate agreement with the measurements, as shown in Table I. Note that there is greater discrepancy between theoretical and measured data for narrow lines than for wide lines. This may be a consequence of the greater dependence of B' values on $\Delta\ell$ for small W/H and therefore a higher reliance on the accuracy of the theoretical $\Delta\ell$ values. Easter's measured data (Fig. 6) suggest that the magnitude of the theoretical $\Delta\ell$ values may in fact be unrealistically high for narrow lines ($W/H < 1$). For the 50-percent miter, susceptance values derived from Campbell's results together with the Babinet equivalence between parallel-plate guide and microstrip again show poor agreement with the measurements.

The frequency variation of the equivalent circuit parameters is measurable, although the magnitude of the variation reported here is typically somewhat greater than that reported by Easter [11]. The only theoretical data available for the dynamic case is that due to Wolff [21] for the 50-Ω bend on alumina, where agreement with measurement is poor (Fig. 5).

V. The Optimum Percentage Miter M

A. Right-Angle Bend, 45° Miter

Fig. 7 indicates the variation in the optimum percentage miter M as a function of linewidth for ε_r values in the range 2.5 to 25. It is remarkable how closely the various points independently of ε_r appear to lie on a single smooth curve described by the following empirical expression:

$$M = 52 + 65 \exp(-1.35 W/H), \qquad W/H \geq 0.25, \quad \varepsilon_r \leq 25. \quad (5)$$

For wide lines, M appears to reach an asymptotic value of approximately 50 percent, although there does not appear to be any obvious physical explanation for this. Over the whole range of parameters investigated the commonly used 50-percent miter never results in over-compensation, invariably providing a better match than for the unmitered case.

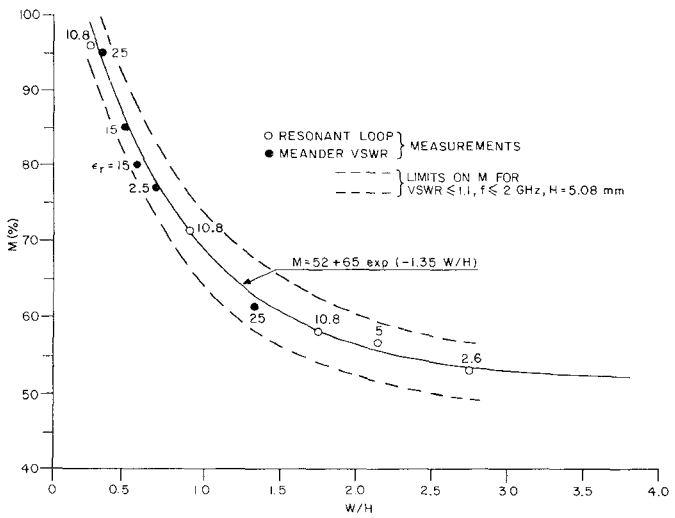

Fig. 7. Optimum miter percentage as a function of normalized linewidth for various ε_r values.

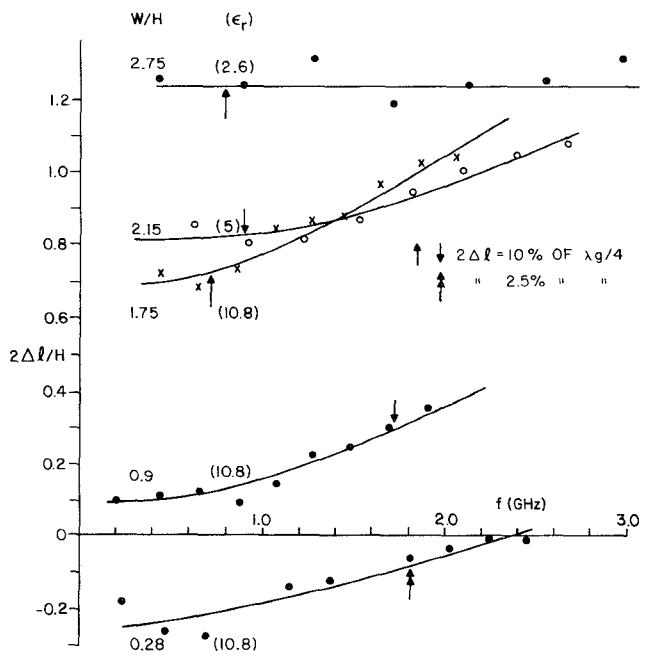

Fig. 8. Frequency dependence of normalized bend electrical length for several optimally mitered configurations.

However, for narrow lines (e.g., 50 Ω on 0.635-mm garnet) the mismatch associated with the 50-percent mitered case is still substantial (Fig. 9(b)).

For lines of nominally 50-Ω characteristic impedance the measured optimum miter for a given ε_r is alternatively available from the following very simple empirical expression

$$M = 46 + 2.5\varepsilon_r, \qquad \varepsilon_r \leq 16, \quad Z_0 \simeq 50\ \Omega. \tag{6}$$

For design purposes, (5) and (6) may be considered to be accurate to ±4, resulting in a maximum VSWR of 1.1 up to 2 GHz ($H = 5$ mm, $W/H \geq 0.25$). These tolerance limits account for curve-fitting and measurement errors as well as the apparent slight sensitivity of the optimum miter to frequency. For narrow lines some care is necessary in fabrication to avoid accidental loss of continuity or over compensation due to poor control of etching.

The frequency variation of the measured normalized bend electrical length, $2\Delta\ell/H$, is shown in Fig. 8 for several optimally mitered configurations of practical significance.

VI. Design Information

This section presents a summary of information useful to the circuit designer who is concerned with accounting for or minimizing the effects of symmetric bends in microstrip.

A. Unmitered Bends

First, an estimate of the low frequency value of the equivalent electrical length $2\Delta\ell$ is obtained from Thomson and Gopinath's curve of Fig. 6 [7] for any given linewidth. With the C_d value obtained from the uniform plane wave model ($C_d = C_\infty W$) and by use of (3), this then yields a low frequency estimate for B'. An indication of the frequency dependence of the circuit elements may be obtained by reference to Table I, Figs. 4 and 5, and [11].

B. Mitered Bends

Over a wide range of ε_r's and normalized linewidths, the optimum miter percentage, M, can be readily calculated from the general expression (5), or for the specific case of 50-Ω lines from (6). These expressions permit the design of bends having maximum VSWR's of 1.1 up to 16 GHz on 0.635-mm substrates.

An estimate of the low frequency value of the electrical length $2\Delta\ell$ for the optimally mitered case may be read from the dotted curve shown in Fig. 6. The frequency dependence of this component may be estimated by reference to Fig. 8.

C. 45 and 60° Bends

Often bends of other than a 90° angle are desirable. Fig. 9(a) presents measured 12-GHz data for B' as a function of percentage miter for the case of a 45° bend in a nominally 50-Ω line on alumina, for which the optimum miter is seen to be approximately 30 percent. It may be useful to note that two unmitered 45° bends used in place of a single unmitered 90° bend always provide a lower mismatch, similar to the experience with stripline [1]. For the corresponding case involving unmagnetized garnet substrates, 60 and 45° bends may be designed by use of the results plotted in Fig. 9(b); the 60° case is particularly useful for circulator designs.

D. Comparison with Published Data

Very few results are available for comparison. The optimum miter percentage given by Kelley *et al.* [12] for a 90° bend in a 50-Ω line on alumina is 57 percent and does not agree well with our observation. However, the measured value of 72 percent reported by Easter *et al.* [10] is in excellent agreement. For $\varepsilon_r = 2.6$ none of the results and trends reported by Hammerstad [14] agree well with our data.

VI. Conclusions

We have described microstrip measurements undertaken using both a resonant-loop technique and a simple return

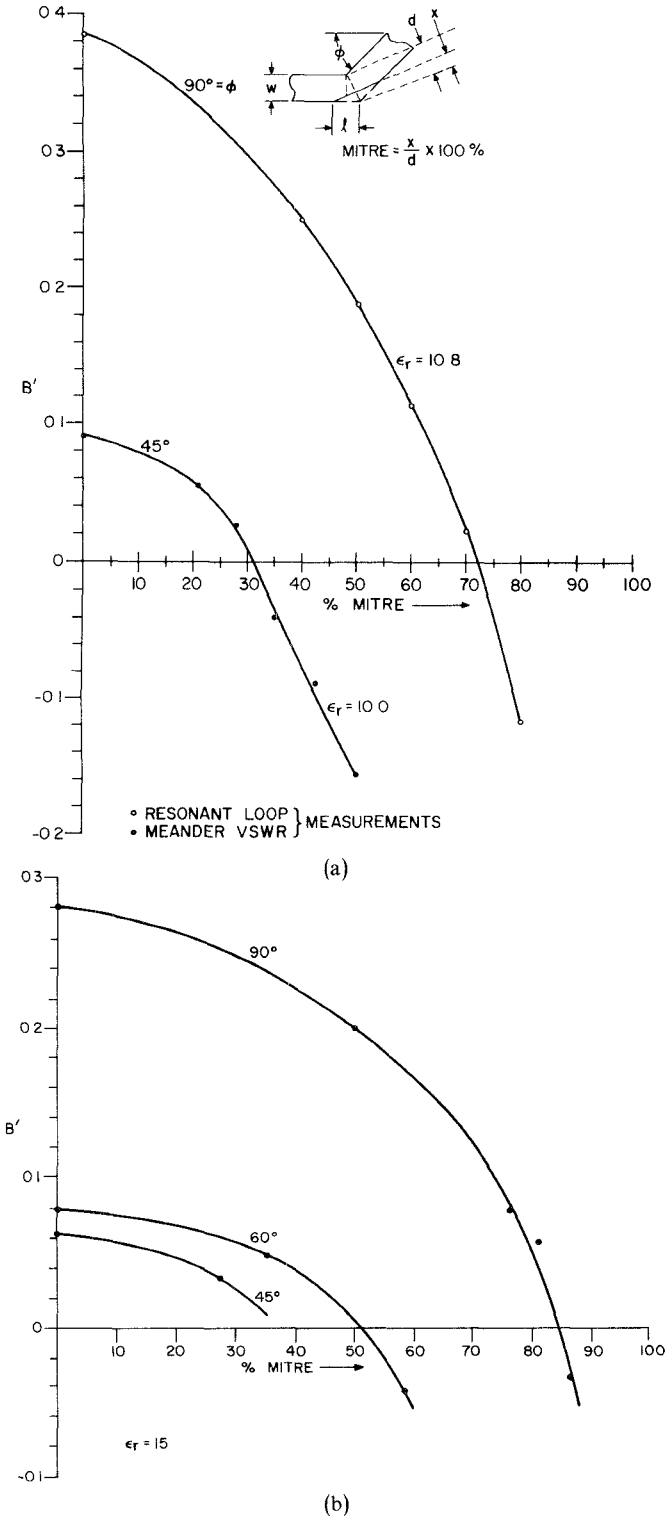

Fig. 9. Variation of normalized susceptance with miter for nominally 50-Ω lines at 12 GHz on 0.635-mm substrates. (a) 90 and 45° bends on alumina. (b) 90, 60, and 45° bends on unmagnetized garnet.

loss method. The 90° bend electrical length and shunt susceptance values have been obtained for a useful range of line widths, dielectric constants and frequencies.

We have investigated the reduction in discontinuity capacitance obtainable by rounding or 45° mitering of the bend and useful empirical expressions have been presented for the optimum miter percentage as functions of linewidth and ε_r. The optimum miter was also determined for 45° bends in 50-Ω line on alumina, and for 45 and 60° bends in 50-Ω line on garnet.

There is generally significant frequency dependence of the elements of the discontinuity equivalent circuit. However, for the unmitered case the experimental data, when extrapolated to zero frequency, agree reasonably well with theoretical results available from quasistatic analyses. There is no theoretical data presently available for mitered configurations.

Acknowledgment

The authors are grateful to R. Marchand, E. Minkus, and N. Morin for performing most of the measurements, and to G. R. Painchaud, F. Bouchard, and M. Stubbs for some of the computed results.

References

[1] H. M. Altschuler and A A. Oliner, "Discontinuities in the center conductor of symmetric strip transmission line," *IRE Trans. Microwave Theory Tech.*, vol. MTT-8, pp. 328–339, May 1960.

[2] A. A. Oliner, "Equivalent circuits for discontinuities in balanced strip transmission line," *IEEE Trans. Microwave Theory Tech.*, vol. MTT-3, pp. 134–143, Mar. 1955.

[3] J J. Campbell, "Application of the solutions of certain boundary value problems to the symmetrical four-port junction and specially truncated bends in parallel-plate waveguides and balanced strip-transmission lines," *IEEE Trans. Microwave Theory Tech.*, vol. MTT-16, pp. 165–176, Mar. 1968.

[4] P. Benedek and P Silvester, "Microstrip discontinuity capacitances for right-angle bends, T junctions, and crossings," *IEEE Trans Microwave Theory Tech.*, vol. MTT-21, pp. 341–346, May 1973.

[5] A. Gopinath and B. Easter, "Moment method of calculating discontinuity inductance of microstrip right-angled bends," *IEEE Trans. Microwave Theory Tech.*, vol. MTT-22, pp. 880–883, Oct. 1974.

[6] R. Horton, "Electrical characterization of a right-angled bend in microstrip line," *IEEE Trans. Microwave Theory Tech.*, vol. MTT-21, pp. 427–429, June 1973.

[7] A. Thomson and A Gopinath, "Calculation of microstrip discontinuity inductances," *IEEE Trans. Microwave Theory Tech.*, vol. MTT-23, pp. 648–655, Aug 1975.

[8] I. Wolff and W. Menzel, "A universal method to calculate the dynamical properties of microstrip discontinuities," presented at *Proc. 5th European Microwave Conf.*, Hamburg, Germany, Sept. 1975.

[9] B. Easter and I. M. Stephenson, "Resonance techniques for establishing the equivalent circuits of small discontinuities in microstrip," *Electron. Lett.*, vol. 7, p. 582, Sept. 1971.

[10] B. Easter, J. G. Richings, and I. M. Stephenson, "Resonant techniques for the accurate measurement of microstrip properties and equivalent circuits," in *Proc. 1973 European Microwave Conf.* (Brussels, Belgium), Paper B.7.5.

[11] B. Easter, "The equivalent circuit of some microstrip discontinuities," *IEEE Trans. Microwave Theory Tech.*, vol. MTT-23, pp. 655–660, Aug. 1975

[12] D. Kelley, A G. Kramer, and F. C. Willwerth, "Microstrip filters and couplers," *IEEE Trans. Microwave Theory Tech.*, vol. MTT-16, pp. 560–562, Aug. 1968.

[13] L. Lewin, "Radiation from discontinuities in striplines," *Inst. Elect. Eng. Monogr.*, no 358E, pp. 163–170, Feb. 1960.

[14] E. O. Hammerstad, "Microstrip handbook," *ELAB Rept.*, no. STF44-A74169, Univ. of Trondheim, Norway, Feb. 1975.

[15] R J. P. Douville and D. S. James, "Experimental characterization of microstrip bends and their frequency dependent behavior," *IEECE 1973 Conf. Digest*, Toronto, Canada, pp. 24–25, Oct. 1973.

[16] W. J. R. Hoefer and A. Chattopadhyay, "Evaluation of the equivalent circuit parameters of microstrip discontinuities through perturbation of a resonant ring," *IEEE Trans. Microwave Theory Tech.*, vol. MTT-23, pp. 1067–1071

[17] E. O. Hammerstad, "Equations for microstrip circuit design," in *Proc. 5th European Microwave Conf.* (Hamburg, Germany), pp. 268–272, Sept. 1975.

[18] W. J. Getsinger, "Microstrip dispersion model," *IEEE Trans. Microwave Theory Tech*, vol. MTT-21, pp. 34–39, Jan. 1973.

[19] J. I. Smith, "The even- and odd-mode capacitance parameters for coupled lines in suspended substrates," *IEEE Trans. Microwave Theory Tech.*, vol. MTT-19, pp. 424–431, May 1971.
[20] W. H. Leighton and A. G. Milnes, "Junction reactance and dimensional tolerance effects on X-band 3-dB directional couplers," *IEEE Trans. Microwave Theory Tech.*, vol. MTT-19, pp. 818–824, Oct. 1971.
[21] I. Wolff, Sept 1975, private communication.
[22] H. J. Schmitt and K. H. Sarges, "Wave propagation in microstrip," *Nachrichtentech Z.*, vol. 24, no. 5, pp. 260–264, 1971.

Some Considerations About the Frequency Dependence of the Characteristic Impedance of Uniform Microstrips

BRUNO BIANCO, LUIGI PANINI, MAURO PARODI, AND SANDRO RIDELLA, MEMBER, IEEE

Abstract—**Various possible definitions of characteristic impedance are derived from two different microstrip models obtaining similar results. It is shown that slightly different definitions yield strongly different behavior versus frequency.**

I. Introduction

THE FREQUENCY DEPENDENCE of the characteristic impedance $Z_0(\omega)$ of uniform microstrips has been discussed in various papers [4]–[10] with completely different results. In Denlinger's approach [4] $Z_0(\omega)$ is a decreasing function, while the other authors have obtained an increasing behavior.

In this paper it is shown how it is possible to obtain such different results, starting from the definitions of voltage, current, and power in microstrip.

Microstrips are transmission lines difficult to analyze. A microstrip, due to the presence of two distinct dielectric media, cannot carry a pure TEM mode. In most practical cases it can be assumed that only one mode (referred to as the fundamental mode) does propagate; however, the pertinent propagation constant γ does not depend linearly on the frequency; this is the dispersion phenomenon. This situation of single-mode propagation is assumed, in general, in the available theoretical calculations. Regarding measurements, γ or $\varepsilon_e = -\gamma^2/\omega^2\varepsilon_0\mu_0$ can be determined by means of techniques which eliminate the effects of the strip terminations, such as the use of sliding probes or by comparing lines of different lengths [11]. This may explain the availability of computations of γ which (with some adjustment of parameters) compare well with measurements [1], [2].

Insofar as the characteristic impedance is concerned, the case is far more involved. Strictly speaking, we could only define the characteristic impedance pertinent to each mode; then when one speaks of the characteristic impedance of the microstrip, it is intended, either explicitly or not, that some hypothesis is made about the mode coupling imposed by the terminations.

The various $Z_0(\omega)$ definable are different. In the present work we shall consider a number of different possible definitions of Z_0, on the basis of two microstrip models, due to W. J. Getsinger and H. J. Carlin, respectively.

II. Getsinger's Model

In this model [1] the microstrip fundamental mode is approximated by a longitudinal-section-electric mode. However, as the actual structure precludes a direct analysis, the microstrip (Fig. 1(a)) is substituted by the structure of Fig. 1(b); here the three unknowns (a', b', and u) are found by supposing that the new structure exhibits the same per-unit-length capacitance and inductance as the original one. A third equation arises when we suppose that the calculated γ fits exactly with a measured value at a given frequency, e.g., at 10 GHz. With this adjustment Getsinger was able to give a good analytical expression for γ. The analysis of the structure of Fig. 1(b) yields [1]:

$$H_{z,i} = -A_i\gamma\gamma_i sh(\gamma_i\psi_i) \tag{1}$$

$$H_{\psi,i} = -A_i\gamma^2 ch(\gamma_i\psi_i) \tag{2}$$

$$E_{\eta,i} = s\mu_0\gamma A_i ch(\gamma_i\psi_i) \tag{3}$$

$$\gamma^2 + \gamma_i^2 = s^2\varepsilon_0\varepsilon_i\mu_0 \tag{4}$$

Manuscript received July 26, 1976; revised July 28, 1977.

B. Bianco and S. Ridella are with the CNR Laboratory for Electronic Circuits, Via all'Opera Pia, 9/b 16145 Genoa, Italy.
L. Panini is with the Marconi Italiana S.p.A., Genova-Cornigliano, Italy
M. Parodi is with the Department of Electrical Engineering, University of Genoa, Viale F. Causa, 13 16145 Genova, Italy.

0018-9480/78/0300-0182$00.75